JACS
JOURNAL OF THE AMERICAN CHEMICAL SOCIETY
pubs.acs.org/JACS

Article

CO_2 Unlocks Reactivity: Boryl Silyl Ketene Acetals Enable Mild and Direct C═C Bond Cleavage

Noel Angel Espinosa-Jalapa, Manuel Kümper, and Jonathan O. Bauer*

Cite This: J. Am. Chem. Soc. 2025, 147, 47573−47583

Read Online

ACCESS | Metrics & More | Article Recommendations | Supporting Information

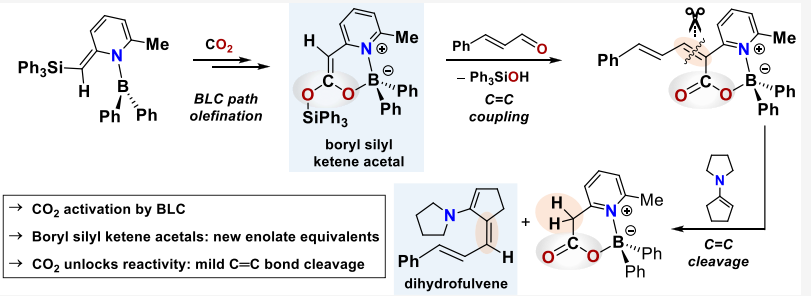

ABSTRACT: Boron−ligand cooperation (BLC) has emerged as a powerful principle of bond activation with main-group elements, yet pyridine-based systems have so far eluded experimental evidence of CO_2 activation. We show here that four-membered pyridyl−boracycles activate CO_2 through a dearomatizing boron−carbon bond cleavage, unambiguously proceeding by a BLC rather than a B/N-FLP-type mechanism, as confirmed by density functional theory (DFT) studies, in contrast to previously predicted computational pathways. This process furnishes boryl silyl ketene acetals, a hitherto unknown class of enolate equivalents in which the two oxygen atoms are differentiated by boryl and silyl substituents. These intermediates exhibit remarkable follow-up reactivity, eventually leading to a mild, one-step C═C double-bond cleavage that delivers fulvene derivatives under additive-free conditions, thereby constituting an unprecedented form of metathesis. Overall, our findings establish boryl silyl ketene acetals derived from CO_2 as a novel class of main-group systems that unlock a reactivity platform with far-reaching synthetic implications.

INTRODUCTION

Element−ligand cooperation has recently emerged as a powerful paradigm for bond activation and catalysis with main-group element compounds.[1−11] In such systems, the main-group element and the surrounding molecular framework (ligand) act in genuine synergy, with the ligand actively engaging in bond activation.[1−3] In analogy to metal−ligand cooperation via aromatization/dearomatization in Milstein's pyridine-based pincer complexes,[12−17] boron−ligand cooperation (BLC) is more specifically defined as the intramolecular interplay of a Lewis-acidic boron center with an aromatic backbone.[2] This unique manifestation of intramolecular frustrated Lewis pairs (FLPs)[18−21] involves a dynamic reorganization of π-electron density within the cooperative motif and a switch from covalent to dative B−X interactions during bond activation.[2]

Following pioneering contributions on cooperative boron−ligand systems,[22−24] pyridine-based boranes have attracted increasing attention as promising metal-free analogues of transition-metal pincer complexes for applications in bond activation processes (Figure 1,A−C).[25] van der Vlugt demonstrated the stabilization of a dearomatized boron−pyridyl complex by intramolecular donor coordination (Figure 1,A),[26] while Milstein and co-workers expanded this concept to explicitly involve the boron center in cooperative bond activation (Figure 1,B).[27] The additional donor side arm essentially "locks" the dearomatized form in both examples A and B. Gellrich subsequently showcased the reversible activation of dihydrogen by pyridonate boranes (Figure 1,C),[28] firmly establishing BLC as part of the catalytic toolbox.[29−33] In parallel, substantial progress has been made in the capture, activation, and chemical utilization of CO_2 using main-group element systems.[34−47] Yet, despite its clear potential also in this area,[48−52] ligand cooperation with main-group elements remains in its infancy. While pyridine-based transition-metal complexes readily mediate small-molecule activation, including CO_2,[53−56] analogous pyridine-based main-group systems have not been realized.

Here, we disclose the first experimental evidence that four-membered pyridyl−boracycles activate CO_2 via a boron−ligand cooperation mechanism. In stark contrast to theoretical

Received: September 23, 2025
Revised: November 24, 2025
Accepted: December 5, 2025
Published: December 15, 2025

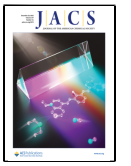

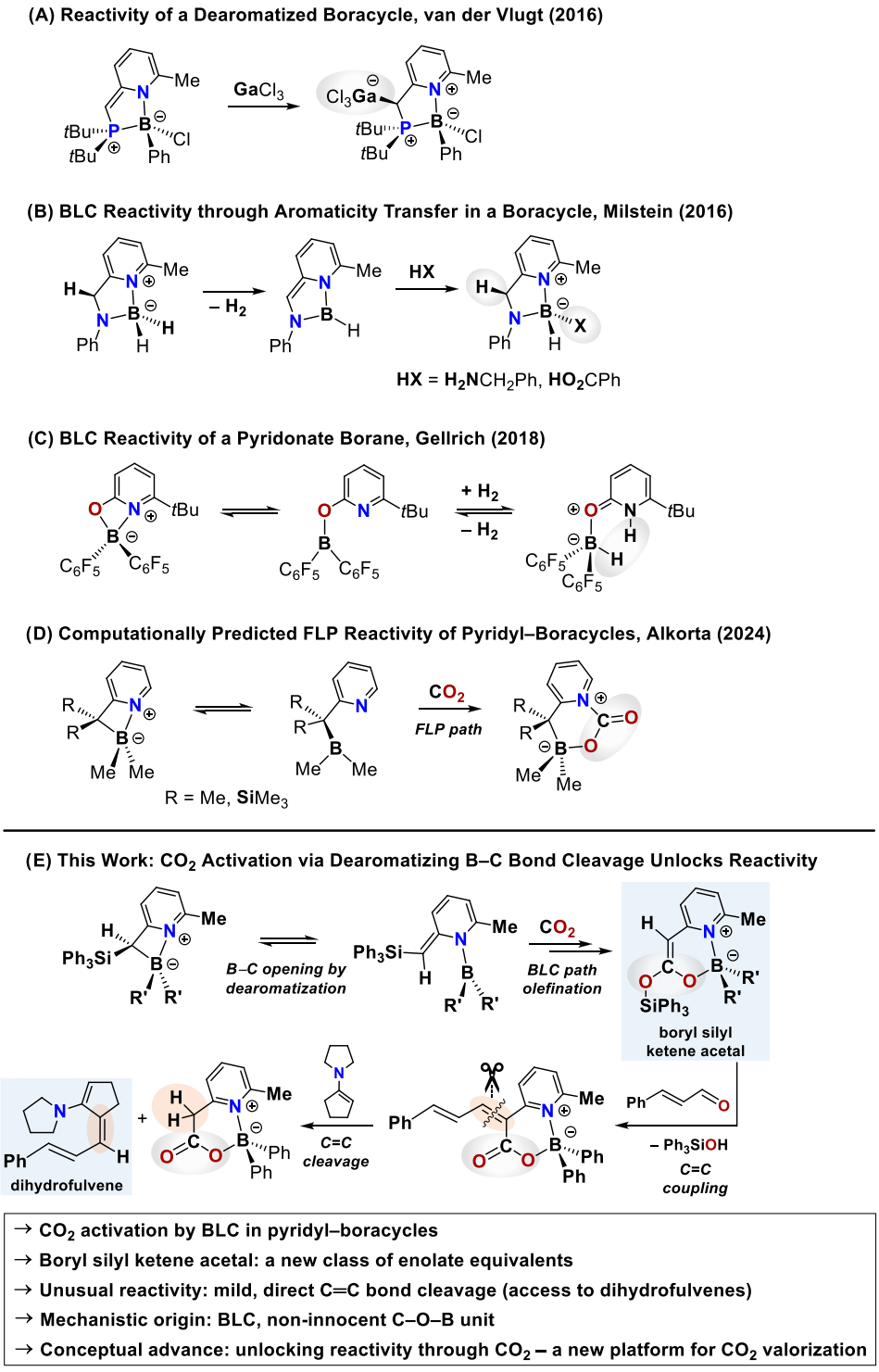

Figure 1. Conceptual development of boron−ligand cooperation (BLC): (A) van der Vlugt's stabilized dearomatized boron−pyridyl complex;[26] (B) Milstein's cooperative boron−ligand system;[27] (C) Gellrich's reversible H_2 activation with pyridonate boranes;[28] (D) Alkorta's theoretical prediction of a B/N-FLP pathway for CO_2 activation;[57] (E) this work: CO_2 activation via dearomatizing B−C bond cleavage furnishes boryl silyl ketene acetals as a new class of enolate equivalents, unlocking exceptional reactivity, including mild and direct C═C double bond cleavage to dihydrofulvenes.

predictions of a B/N-FLP-type pathway (Figure 1,D),[57] the activation proceeds unambiguously via a dearomatizing boron−carbon bond cleavage (Figure 1,E). Complementary density functional theory (DFT) studies reveal that the BLC pathway is strongly favored, both kinetically and thermodynamically, over any conceivable FLP-type mechanism. This unprecedented mode of CO_2 fixation directly furnishes boryl silyl ketene acetals (which can also be viewed as boryl silyl ester enolates), a novel class of enolate equivalents that display a reactivity pattern far beyond that of classical enol or enolate chemistry. Remarkably, these intermediates not only undergo transformations such as Michael- and aldol-type reactions, but

https://doi.org/10.1021/jacs.5c16770
J. Am. Chem. Soc. 2025, 147, 47573−47583

Scheme 1. Synthesis of the Four-Membered Pyridyl−Boracycles 3 and 4 via the Fully Dearomatized Lithium Enamide 2. Ipc = (−)-*iso*-Pinocampheyl

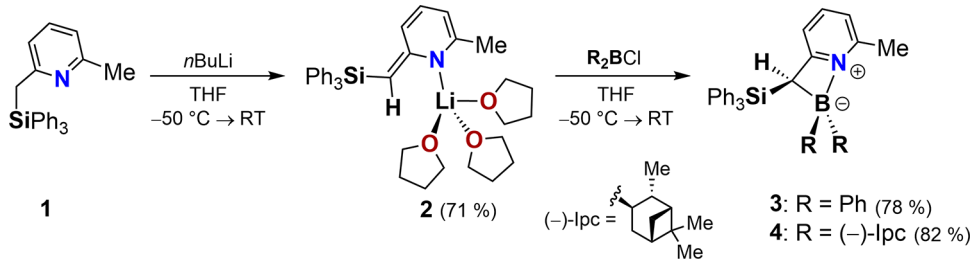

ultimately enable a mild, direct cleavage of a C=C double bond, providing straightforward access to fulvene derivatives.

Taken together, our findings illustrate how BLC drives the formation of unprecedented intermediates. In particular, they establish boryl silyl ketene acetals derived from CO_2 as a novel class of main-group systems that unlock a previously inaccessible reactivity platform.

RESULTS AND DISCUSSION

Evidence of Boron−Ligand Cooperation and Formation of Boryl Silyl Ketene Acetals from CO_2. Building on the potential of small-ring systems[58] and our previous contributions in this field,[59−62] we have now extended our investigations to four-membered pyridine-based boracycles (Figure 1,E). The conjugated π-system in these scaffolds displays striking electronic parallels to the much-discussed bonding motifs in 2-picolyllithium[63−65] and its 2-silylmethyl derivatives,[66−70] to alkali-metal dihydropyridines,[71−75] and to the pyridine backbone of pincer-type complexes.[12−18,25] Reaction pathways in such boracycles, whether following a frustrated Lewis pair (FLP) or a boron−ligand cooperation (BLC) mechanism, have long been debated, and are known to be highly sensitive to the substitution pattern.[76−79]

The synthesis of the target pyridyl−boracycles commenced from 2-(triphenylsilyl)lutidine (**1**) (for the X-ray structural analysis of **1**, see the Supporting Information, SI), which, after lithiation with *n*-butyllithium in tetrahydrofuran (THF), afforded the solvated enamide **2** as single crystals suitable for X-ray diffraction analysis (Scheme 1).

The molecular structure of **2** clearly demonstrates the pronounced disruption of the aromatic π-system (Figure 2). In contrast to previously reported 2-picolyl alkali-metal complexes,[63−70] the lithium cation exhibits no interaction with the aromatic π-system, neither in a carbanionic nor an azaallyl-type fashion. Instead, the coordination is exclusively through the enamide functionality, accompanied by shortened C19−C20 bond lengths [1.395 Å and 1.397 Å (**2**) versus 1.505 Å (**1**)], which are much closer to typical C(sp^2)=C(sp^2) double bonds.[80] The alternating C−C bond lengths in the pyridine ring of **2** (values between 1.361 and 1.443 Å) further corroborate a loss of aromaticity (for comparison, the average C−C bond length in **1** is 1.383 Å). These features already point to a strong predisposition of the ligand framework toward the formation of dearomatized, highly reactive species.

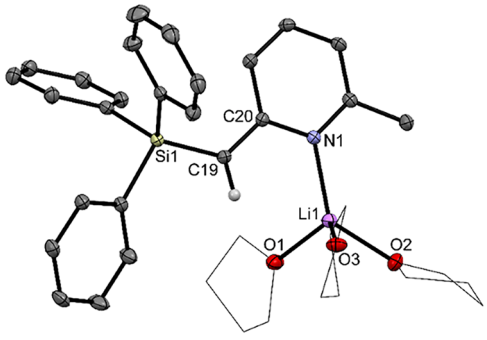

Figure 2. Molecular structure of compound **2** in the crystal (displacement ellipsoids at 50% probability). One molecule of the asymmetric unit is shown. Hydrogen atoms, except H at C19, are omitted for clarity.

Subsequent reaction of **2** with chlorodiphenyl- or chlorodi(−)-*iso*-pinocampheylborane directly afforded monomeric cyclic pyridyl boranes **3** and **4** (Scheme 1), both of which were structurally characterized by single-crystal X-ray diffraction analysis (Figure 3). Compounds **3** and **4** adopt almost perfectly planar four-membered ring geometries, and the boron atoms exhibit a pronounced tetrahedral character, with THCs of 80% (**3**) and 77% (**4**), respectively. The C19−C20 bond lengths of 1.499 Å (**3**) and 1.495 Å (**4**) are in the expected range of C(sp^3)−C(aryl) single bonds[80] [C19−C20 (**1**): 1.505 Å], while the C19−B1 distances are nearly identical across both species (1.705−1.709 Å). Notably, the dative B1−N1 bond in **4** (1.703 and 1.720 Å) is elongated compared to that in **3** (1.643 Å), a consequence of the steric demand imposed by the chiral (−)-*iso*-pinocampheyl substituents.

At room temperature, neither **3** nor **4** showed any reactivity toward CO_2 (3 bar). Upon heating to 90−120 °C in toluene, however, both underwent clean conversion to crystalline products **5** and **6** (Scheme 2), which were unequivocally identified by single-crystal X-ray diffraction analysis as unsaturated six-membered heterocycles (Figure 4). To the best of our knowledge, this transformation represents the first direct entry into boryl silyl ketene acetals, a previously unknown class of compounds. Mechanistically, their formation requires a three-step sequence: (i) dearomatizing cleavage of the B−C bond with formation of intermediates **3′** and **4′**, (ii) CO_2 capture via boron−ligand cooperation, and (iii) an olefination of the α-silyl carboxyl intermediates **7** and **8** triggered by a [1,3]-silyl migration,[81,82] which provides a substantial thermodynamic driving force for the process (Scheme 2).

The structural parameters of **5** and **6** are fully consistent with their assignment as boryl silyl ketene acetals (Figure 4). Their C19−C20 bonds [1.353 Å (**5**), 1.356 Å (**6**)] clearly fall within the range of C(sp^2)=C(sp^2) double bonds of enol esters,[80] corroborating the enolate-like character of these species. In both compounds, the C19−O2 bond [1.303 Å (**5**), 1.290 Å (**6**)] is shorter than the corresponding C19−O1 bond [1.333 Å (**5**), 1.337 Å (**6**)], providing clear structural evidence

https://doi.org/10.1021/jacs.5c16770
J. Am. Chem. Soc. 2025, 147, 47573−47583

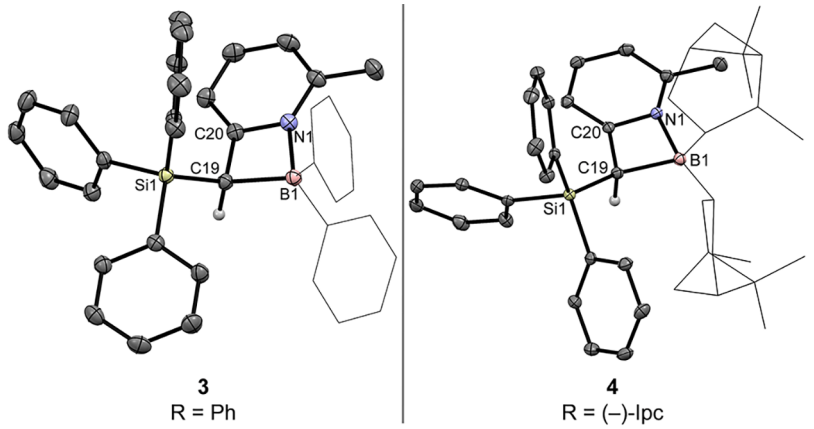

Figure 3. Molecular structures of the pyridyl–boracycles **3** and **4** in the crystal (displacement ellipsoids at 50% probability). One molecule of the asymmetric unit of **4** is shown. Solvent molecules (diethyl ether in **3**) and hydrogen atoms, except H at C19, are omitted for clarity.

Scheme 2. Reaction of Pyridyl–Boracycles 3 and 4 with CO_2 to Give Boryl Silyl Ketene Acetals 5 and 6 via a BLC Mechanism Followed by an Immediate [1,3]-Silyl Migration

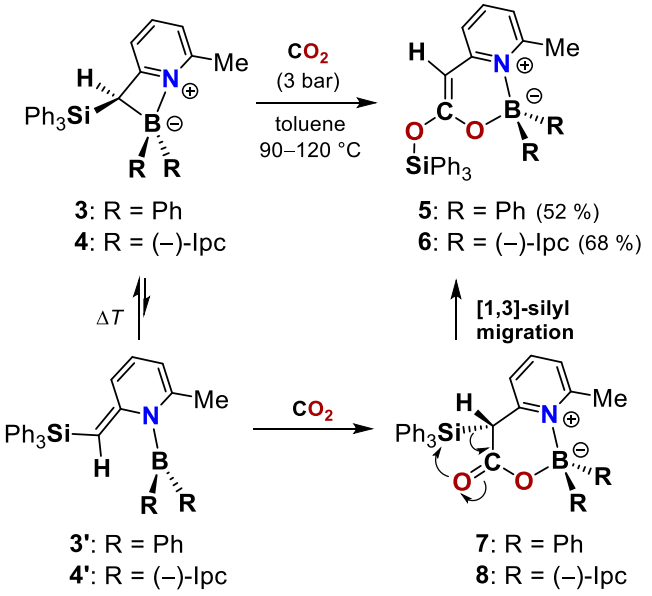

that O2 exerts the stronger +M effect.[83] This differentiation can be rationalized by negative hyperconjugation of the O1 lone pairs with vicinal, antibonding $\sigma^*_{(Si-C)}$ orbitals,[84−86] which stabilizes electron density at O1, whereas such an interaction is negligible for the tetracoordinate second-row element boron, rendering O2 the more effective electron-pair donor in enolate-type reactivity. Notably, the B1−N1 bond in **6** (1.679 Å) is again elongated relative to that in **3** (1.623 Å), highlighting the structural flexibility of the boracyclic framework and its capacity to adapt its bonding interactions in response to reaction demands.

Mechanistic Investigations: BLC Versus B/N-FLP Pathway. To gain deeper insight into the reaction pathway, which our experimental data had already indicated to follow a boron−ligand cooperation (BLC) mechanism, we performed detailed DFT calculations at the M06-2X/6−311+G(d,p) level of theory[87−91] with solvation modeled by the polarizable continuum model (PCM) (solvent: toluene) (Figure 5).[92] Previous theoretical work by Alkorta et al. had suggested an alternative FLP-type pathway, initiated by opening of the B−N bond in the boracycle and followed by exergonic adduct formation between the boron/nitrogen Lewis pair and CO_2.[57] We therefore examined both scenarios (BLC and FLP) in parallel.

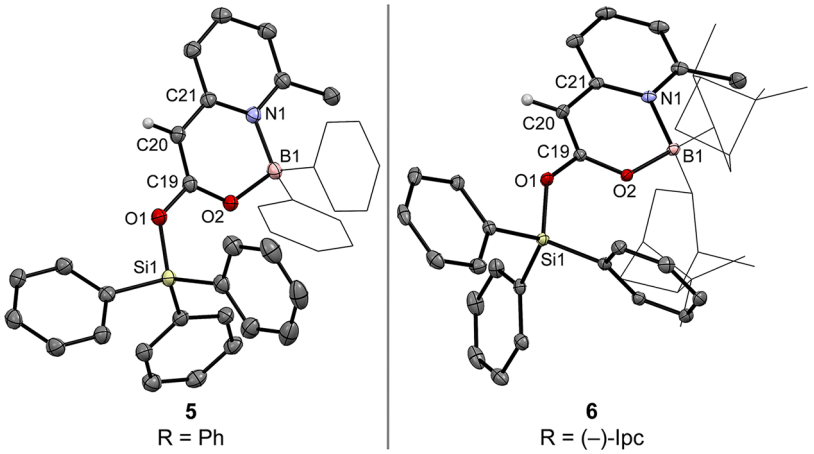

Figure 4. Molecular structures of the boryl silyl ketene acetals **5** and **6** in the crystal (displacement ellipsoids at 50% probability). Solvent molecules (benzene in **5**) and hydrogen atoms, except H at C20, are omitted for clarity.

https://doi.org/10.1021/jacs.5c16770
J. Am. Chem. Soc. 2025, 147, 47573−47583

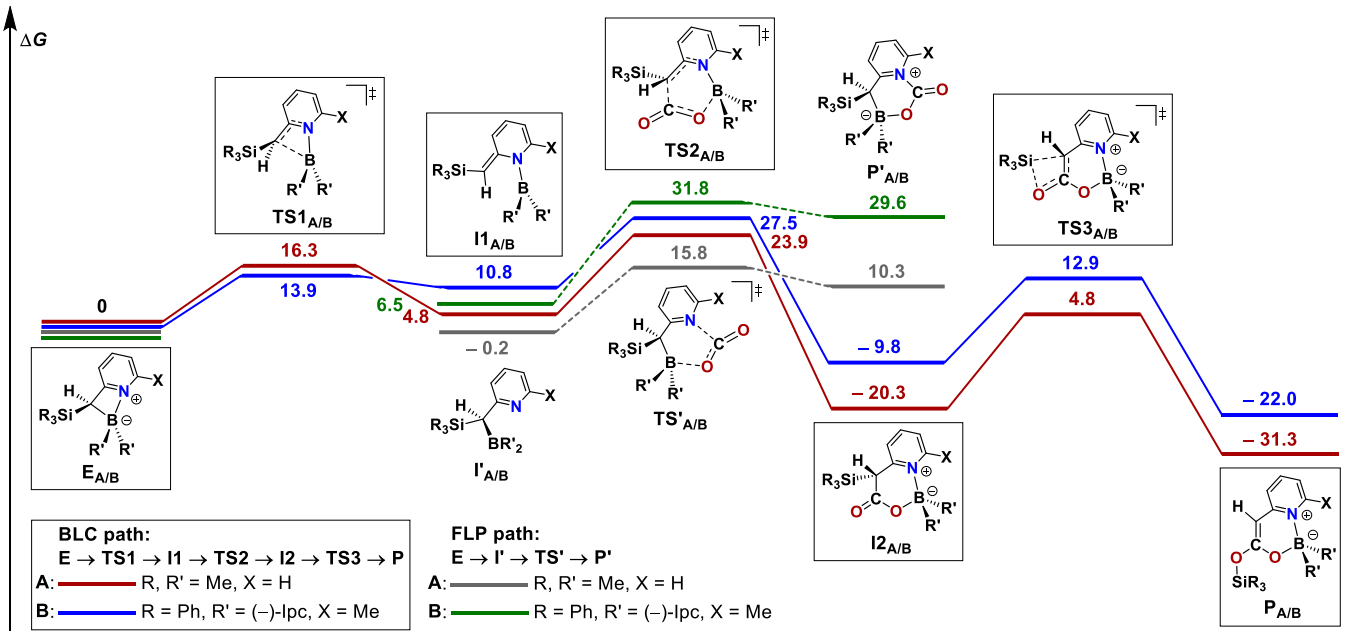

Figure 5. Computed mechanism of CO_2 activation at the M06-2X/6−311+G(d,p) level of theory (PCM, toluene).[87−92] Comparison of the BLC pathway (red/blue) with the B/N-FLP pathway (gray/green). Gibbs energies (ΔG) in kcal mol^{-1}.

Scheme 3. Reaction of Boryl Silyl Ketene Acetal 5 with Acrolein to Give Product 9: Michael-Type Addition Facilitated by the C−O−B Fragment[a]

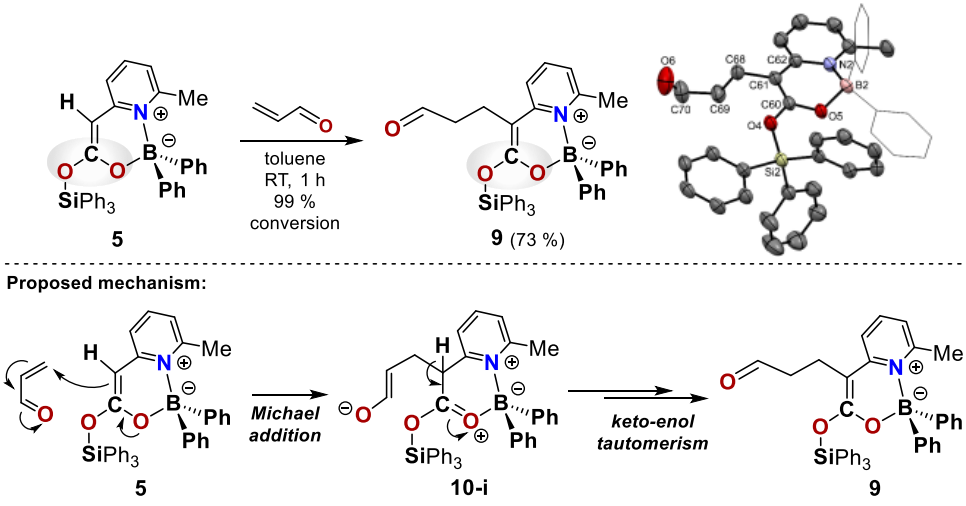

[a]Molecular structure of compound **9** in the crystal (displacement ellipsoids at 50% probability). One molecule of the asymmetric unit is shown. Hydrogen atoms are omitted for clarity.

Calculations were carried out for a simplified 2-picolylborane model system (**A**: R, R′ = Me, X = H) as well as for the experimentally studied 2-lutidylborane (**B**: R = Ph, R′ = (−)-Ipc, and X = Me). In the BLC pathway (red and blue traces, Figure 5), CO_2 activation is initiated by dearomatizing cleavage of the B−C bond, giving the open enamide **I1** via transition state **TS1**. The activation barriers ($\Delta\Delta G^{\ddagger}$) are modest and comparable for both systems (**TS1**$_A$: 16.3 kcal mol^{-1}; **TS1**$_B$: 13.9 kcal mol^{-1}). However, the relative stabilities of the dearomatized intermediates **I1** depend sensitively on the substitution pattern: effective $n_N \rightarrow p_B$ conjugation lowers the energy of **I1**$_A$ (4.8 kcal mol^{-1}), whereas steric congestion from the bulky (−)-*iso*-pinocampheyl substituents destabilizes **I1**$_B$ (10.8 kcal mol^{-1}).

Subsequent attack of CO_2 at open boryl enamide **I1** proceeds through **TS2**$_A$ ($\Delta\Delta G^{\ddagger}$ = 19.1 kcal mol^{-1}) or **TS2**$_B$ ($\Delta\Delta G^{\ddagger}$ = 16.7 kcal mol^{-1}), forming a six-membered cyclic boryl ester intermediate (**I2**). Although **I2** is only transient, its formation is highly exergonic ($\Delta\Delta G$ = −25.1 kcal mol^{-1} for **A**; $\Delta\Delta G$ = −20.6 kcal mol^{-1} for **B**), driven by the restoration of aromaticity. The overall process gains its large thermodynamic driving force (**P**$_A$: ΔG = −31.3 kcal mol^{-1}; **P**$_B$: ΔG = −22.0 kcal mol^{-1}) from the final, rate-determining olefination (**I2**$_{A/B}$ → **P**$_{A/B}$). This step involves a concerted [1,3]-silyl migration proceeding through a four-membered cyclic transition state (**TS3**$_A$: $\Delta\Delta G^{\ddagger}$ = 25.1 kcal mol^{-1}; **TS3**$_B$: $\Delta\Delta G^{\ddagger}$ = 22.7 kcal mol^{-1}), thereby confirming Kira's findings,[93] which is driven by Si−O bond formation and accompanied by the generation of a synthetically valuable, electron-rich ketene-like C═C

https://doi.org/10.1021/jacs.5c16770
J. Am. Chem. Soc. 2025, 147, 47573−47583

Scheme 4. Reaction of Boryl Silyl Ketene Acetal 5 with Cinnamaldehyde: Mukaiyama-Type Aldol Addition Followed by Condensation to the Diastereomers *Z*-11 and *E*-11[a]

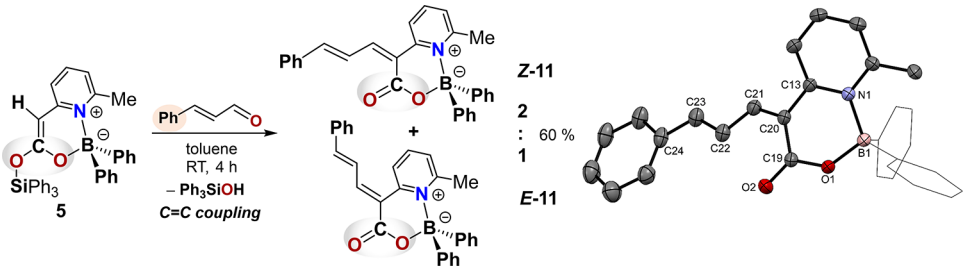

[a]Molecular structure of boryl ester ***Z*-11** in the crystal (displacement ellipsoids at 50% probability). Hydrogen atoms are omitted for clarity.

Scheme 5. C═C Bond Cleavage of *Z*/*E*-11 (2:1) (Only the *Z* Isomer is Shown) with 1-(1-Cyclopent-1-enyl)pyrrolidine: Formation of Reduced Boryl Ester 12 and 3,4-Dihydrofulvene 13[a]

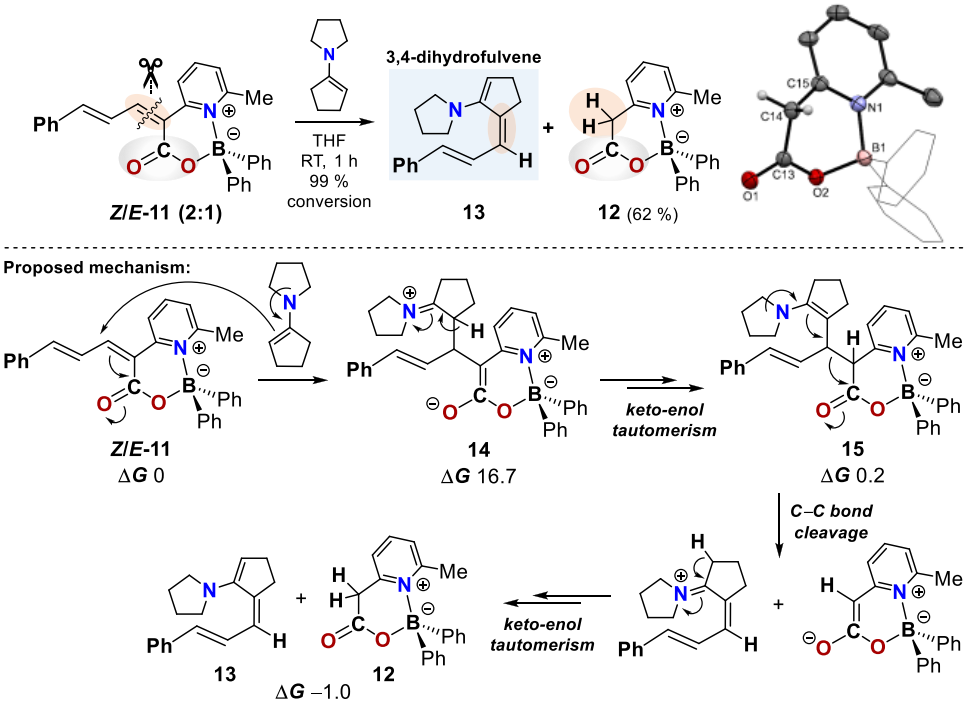

[a]Molecular structure of compound **12** in the crystal (displacement ellipsoids at 50% probability). Hydrogen atoms, except H at C14, are omitted for clarity. Gibbs energies (ΔG, in kcal mol^{-1}) for key species along the reaction pathway were computed at the M06-2X/6−311+G(d,p) level of theory.

double bond (Figure 5). Notably, examples of C−C bond formation with CO_2 in boron/carbon FLP systems are rare, emphasizing the distinctive reactivity of the present BLC system.[34,35,51]

In stark contrast, the alternative FLP pathway (gray and green traces; Figure 5) yields no feasible solution. According to our calculations, formation of a CO_2 adduct from a putative frustrated B/N Lewis pair ($\mathbf{I'}_{A/B} \rightarrow \mathbf{P'}_{A/B}$) is strongly endergonic ($\Delta\Delta G$ = 23.1 and 10.5 kcal mol^{-1} for **A** and **B**, respectively) and does not produce a thermodynamically stable species. The transition states ($\mathbf{TS'}_A$: $\Delta\Delta G^{\ddagger}$ = 16.0 kcal mol^{-1}; $\mathbf{TS'}_B$: $\Delta\Delta G^{\ddagger}$ = 25.3 kcal mol^{-1}) are even higher in energy or at least in a similar range than the corresponding BLC transition states, rendering the FLP scenario highly unlikely (computational results for the bis-silyl-substituted model system are provided in Figure S84 of the SI).

Overall, these computational results are in full agreement with the experiment and demonstrate that CO_2 activation in pyridyl−boracycles proceeds unequivocally via a BLC mechanism. Importantly, this holds true irrespective of the specific substituents present at the 6-position of the pyridine ring or within the silyl and boryl groups, indicating the generality and robustness of this cooperative activation mode.

Follow-Up Reactions (Michael and Aldol Reactions) of the Boryl Silyl Ketene Acetals. The products of CO_2 activation constitute a previously unknown class of enolate equivalents, distinguished by a unique bifunctional motif in which one oxygen atom is bound to a silyl group and the other to a boryl substituent. Owing to the embedding of the electron-rich olefinic unit within a rigid cyclic framework, we next probed their dienophilicity. As electron-deficient reaction partners for a potential inverse-electron-demand hetero-Diels−Alder (iEDHDA) reaction,[94−99] acrolein and cinnamaldehyde were selected (Schemes 3 and 4). Reaction with acrolein (Scheme 3) did not proceed via a concerted [4 + 2] cycloaddition but instead followed a stepwise pathway. The

https://doi.org/10.1021/jacs.5c16770
J. Am. Chem. Soc. 2025, 147, 47573−47583

initial Michael-type 1,4-addition is facilitated by the C−O−B fragment, which acts as a noninnocent cooperative motif, with its pronounced +M effect playing a decisive role.[83] The resulting zwitterionic intermediate **10-i** is stabilized through proton abstraction and subsequent keto−enol tautomerization (Scheme 3, bottom). Steric constraints render a ring closure via intramolecular attack of the alkoxide at the activated carboxyl carbon atom of **10-i** implausible. Remarkably, the transformation does not follow a Mukaiyama−Michael pathway either;[100−103] instead, the ketene acetal functionality in **9** remains entirely intact.

In sharp contrast, the reaction of **5** with cinnamaldehyde follows a different trajectory (Scheme 4). Here, a C═C coupling reaction occurs that can be interpreted as a Lewis-acid-free, Mukaiyama-type aldol addition[104−106] followed by condensation under mild conditions, affording the two diastereomers ***Z*-11** and ***E*-11** in a 2:1 ratio. We attribute this unusually mild, additive-free reactivity to the unique dual character of our boryl silyl ketene acetals, which merge key features of both boron and silicon enolates.[107−109] In contrast to classical Lewis-acid-promoted Mukaiyama aldol reactions, which are generally assumed to proceed via an open transition state,[110−112] the present addition most plausibly follows a closed, Zimmerman−Traxler-type chairlike transition state,[113] in which a pentacoordinate silicon atom constitutes an integral part of the cyclic transition-state framework (for mechanistic details supported by DFT calculations, see Figure S85 in the SI). Subsequent elimination of Ph_3SiOH likely occurs from the enol form via a hydrogen-bonded transition state. The observed *Z*:*E* ratio can be rationalized by differences in the activation barriers of the two diastereomeric transition states, arising after rotation around the C(α)−C(β) bond in the enolic intermediate (see Section S5 in the SI).

Mild, Direct C═C Bond Cleavage Enabling Access to Fulvene Derivatives. The selective scission of C═C double bonds is of fundamental importance in synthetic organic chemistry.[114,115] In addition to olefin metathesis,[116,117] the oxidative cleavage of alkenes into valuable carbonyl compounds represents one of the most widely applied and most actively explored transformations.[118−125] Against this backdrop, the discovery of a mild approach to C═C bond cleavage, providing direct access to previously inaccessible classes of compounds, is highly significant.

Given that the $\alpha,\beta,\gamma,\delta$-unsaturated boryl esters ***Z*-11** and ***E*-11** possess an electron-deficient diene framework, we next explored their reactivity in the context of a hetero-Diels−Alder reaction with inverse electron demand, employing an enamine as an electron-rich dienophile. Strikingly, rather than proceeding through an iEDHDA pathway, the reaction follows an entirely unanticipated course, resulting in novel, mild, and direct C═C bond cleavage (Scheme 5).

Treatment of the ***Z*/*E*-11** isomer mixture (2:1) with 1-(1-cyclopent-1-enyl)pyrrolidine at room temperature resulted in complete conversion (99%) and afforded reduced cyclic boryl ester **12** in 62% isolated yield, which was fully characterized by single-crystal X-ray diffraction analysis. Retrosynthetic analysis a priori suggested the concomitant formation of a 3,4-dihydrofulvene (**13**) (Scheme 5, bottom), which was indeed confirmed by NMR spectroscopy and high-resolution mass spectrometry (HRMS), even though isolation proved unfeasible owing to its pronounced tendency toward polymerization.

The mechanistic sequence begins with the formation of the zwitterionic iminium intermediate **14**, which undergoes proton elimination followed by keto−enol tautomerization rather than ring closure. The resulting enamine intermediate **15** promotes C−C bond cleavage, and subsequent proton transfer reactions furnish products **12** and **13**. In this process, a new C═C bond is formed as the exocyclic double bond of 3,4-dihydrofulvene, bearing an electron-donating substituent at its 1-position. Accordingly, this transformation can be regarded as a new type of metathesis reaction.

Moreover, the facile recovery of compound **5**, directly accessible from compound **12**, underlines its potential as a sustainable auxiliary in preparative chemistry (for details, see Section S3 in the SI).

In sum, these findings establish cyclopentenylamines as hitherto unknown cleavage reagents that enable direct access to fulvene derivatives, a synthetically valuable class of compounds with a uniquely rich reactivity profile, whose preparation has always been challenging.[126−130] This discovery not only expands the scope of boron−ligand cooperation chemistry but also highlights a conceptually new strategy for selective C═C bond scission under remarkably mild conditions. Ongoing studies are directed toward probing the synthetic potential and extending this methodology to diverse substitution patterns.

CONCLUSIONS

This work establishes boryl silyl ketene acetals derived from CO_2 as a previously unexplored class of main-group intermediates with unique reactivity. We provide the first experimental evidence that pyridyl−boracycles activate CO_2 through a boron−ligand cooperation (BLC) mechanism rather than via a B/N-FLP-type pathway. Crucially, CO_2 is not merely sequestered but initiates a reaction cascade, leading to boryl silyl ketene acetals. These intermediates display a strikingly broad spectrum of unforeseen follow-up reactivity, including Michael- and aldol-type reactions, and ultimately leading to a mild, one-step cleavage of C═C double bonds that affords fulvene derivatives under additive-free conditions. Collectively, CO_2 capture by pyridyl−boracycles enables entirely new reactivity patterns and synthetic strategies far beyond classical enolate or enol chemistry, thereby opening new conceptual and synthetic perspectives for main-group element chemistry. All transformations of the boryl silyl ketene acetals proceed under mild conditions, in the absence of additives, and with high chemoselectivity, which are features that underscore the robustness and versatility of this platform. We attribute this behavior to the unusual combination of a rigid yet electronically adaptive cyclic framework with the cooperative interplay between the keto and enolate forms of the C−O−B functionality.

ASSOCIATED CONTENT

Supporting Information

The Supporting Information is available free of charge at https://pubs.acs.org/doi/10.1021/jacs.5c16770.

Synthetic procedures; NMR spectra of all isolated compounds; and detailed information on X-ray crystallography and quantum chemical calculations (PDF)

Accession Codes

Deposition Numbers 2483841−2483849 contain the supplementary crystallographic data for this paper. These data can be obtained free of charge via the joint Cambridge Crystallo-

https://doi.org/10.1021/jacs.5c16770
J. Am. Chem. Soc. 2025, 147, 47573−47583

graphic Data Centre (CCDC) and Fachinformationszentrum Karlsruhe Access Structures service.

AUTHOR INFORMATION

Corresponding Author

Jonathan O. Bauer − *Faculty of Chemistry and Pharmacy, Institute of Inorganic Chemistry, University of Regensburg, D-93053 Regensburg, Germany;* orcid.org/0000-0002-9575-7430; Email: jonathan.bauer@ur.de

Authors

Noel Angel Espinosa-Jalapa − *Faculty of Chemistry and Pharmacy, Institute of Inorganic Chemistry, University of Regensburg, D-93053 Regensburg, Germany*

Manuel Kümper − *Faculty of Chemistry and Pharmacy, Institute of Inorganic Chemistry, University of Regensburg, D-93053 Regensburg, Germany*

Complete contact information is available at: https://pubs.acs.org/10.1021/jacs.5c16770

Notes

The authors declare no competing financial interest.

ACKNOWLEDGMENTS

J.O.B. thanks the Elite Network of Bavaria (ENB) and the Bavarian State Ministry of Science and the Arts (StMWK) for financial support (Project N-LW-NW-2016-366). Further support was provided by the Deutsche Forschungsgemeinschaft (DFG, German Research Foundation) through the Research Training Group "Ion Pair Effects in Molecular Reactivity" (RTG 2620, Project 426795949). M.K. thanks the Fonds der Chemischen Industrie (FCI) for a Kekulé fellowship.

REFERENCES

(1) Greb, L.; Ebner, F.; Ginzburg, Y.; Sigmund, L. M. Element-Ligand Cooperativity with p-Block Elements. *Eur. J. Inorg. Chem.* **2020**, *2020*, 3030−3047.

(2) Hasenbeck, M.; Gellrich, U. Boron−Ligand Cooperation: The Concept and Applications. *Chem. − Eur. J.* **2021**, *27*, 5615−5626.

(3) Montag, M.; Milstein, D. Catalytic Main-Group Metal Complexes of Phosphine-Based Pincer Ligands. *Isr. J. Chem.* **2023**, *63*, No. e202300082.

(4) Myers, T. W.; Berben, L. A. Aluminum−Ligand Cooperative N−H Bond Activation and an Example of Dehydrogenative Coupling. *J. Am. Chem. Soc.* **2013**, *135*, 9988−9990.

(5) Abdalla, J. A. B.; Riddlestone, I. M.; Tirfoin, R.; Aldridge, S. Cooperative Bond Activation and Catalytic Reduction of Carbon Dioxide at a Group 13 Metal Center. *Angew. Chem., Int. Ed.* **2015**, *54*, 5098−5102.

(6) Ebner, F.; Sigmund, L. M.; Greb, L. Metal−Ligand Cooperativity of the Calix[4]pyrrolato Aluminate: Triggerable C−C Bond Formation and Rate Control in Catalysis. *Angew. Chem., Int. Ed.* **2020**, *59*, 17118−17124.

(7) Sigmund, L. M.; Ehlert, C.; Enders, M.; Graf, J.; Gryn'ova, G.; Greb, L. Dioxygen Activation and Pyrrole α-Cleavage with Calix[4]-pyrrolato Aluminates: Enzyme Model by Structural Constraint. *Angew. Chem., Int. Ed.* **2021**, *60*, 15632−15640.

(8) Liang, Y.; Das, U. K.; Luo, J.; Diskin-Posner, Y.; Avram, L.; Milstein, D. Magnesium Pincer Complexes and Their Applications in Catalytic Semihydrogenation of Alkynes and Hydrogenation of Alkenes: Evidence for Metal−Ligand Cooperation. *J. Am. Chem. Soc.* **2022**, *144*, 19115−19126.

(9) Liang, Y.; Luo, J.; Diskin-Posner, Y.; Milstein, D. Designing New Magnesium Pincer Complexes for Catalytic Hydrogenation of Imines and *N*-Heteroarenes: H_2 and N−H Activation by Metal−Ligand Cooperation as Key Steps. *J. Am. Chem. Soc.* **2023**, *145*, 9164−9175.

(10) Yadav, R.; Janßen, P.; Schorpp, M.; Greb, L. Calix[4]pyrrolato-germane-$(thf)_2$: Unlocking the Anti-van't Hoff−Le Bel Reactivity of Germanium(IV) by Ligand Dissociation. *J. Am. Chem. Soc.* **2023**, *145*, 17746−17754.

(11) Liang, Y.; Efremenko, I.; Diskin-Posner, Y.; Avram, L.; Milstein, D. Calcium-Ligand Cooperation Promoted Activation of N_2O, Amine, and H_2 as well as Catalytic Hydrogenation of Imines, Quinoline, and Alkenes. *Angew. Chem., Int. Ed.* **2024**, *63*, No. e202401702.

(12) Gunanathan, C.; Milstein, D. Bond Activation and Catalysis by Ruthenium Pincer Complexes. *Chem. Rev.* **2014**, *114*, 12024−12087.

(13) Khusnutdinova, J. R.; Milstein, D. Metal−Ligand Cooperation. *Angew. Chem., Int. Ed.* **2015**, *54*, 12236−12273.

(14) Zhang, J.; Leitus, G.; Ben-David, Y.; Milstein, D. Facile Conversion of Alcohols into Esters and Dihydrogen Catalyzed by New Ruthenium Complexes. *J. Am. Chem. Soc.* **2005**, *127*, 10840−10841.

(15) Ben-Ari, E.; Leitus, G.; Shimon, L. J. W.; Milstein, D. Metal−Ligand Cooperation in C−H and H_2 Activation by an Electron-Rich PNP Ir(I) System: Facile Ligand Dearomatization−Aromatization as Key Steps. *J. Am. Chem. Soc.* **2006**, *128*, 15390−15391.

(16) Gunanathan, C.; Ben-David, Y.; Milstein, D. Direct Synthesis of Amides from Alcohols and Amines with Liberation of H_2. *Science* **2007**, *317*, 790−792.

(17) van der Vlugt, J. I.; Reek, J. N. H. Neutral Tridentate PNP Ligands and Their Hybrid Analogues: Versatile Non-Innocent Scaffolds for Homogeneous Catalysis. *Angew. Chem., Int. Ed.* **2009**, *48*, 8832−8846.

(18) Habraken, E. R. M.; Jupp, A. R.; Brands, M. B.; Nieger, M.; Ehlers, A. W.; Slootweg, J. C. Parallels between Metal-Ligand Cooperativity and Frustrated Lewis Pairs. *Eur. J. Inorg. Chem.* **2019**, *2019*, 2436−2442.

(19) Welch, G. C.; San Juan, R. R.; Masuda, J. D.; Stephan, D. W. Reversible, Metal-Free Hydrogen Activation. *Science* **2006**, *314*, 1124−1126.

(20) Mömming, C.; Otten, E.; Kehr, G.; Fröhlich, R.; Grimme, S.; Stephan, D. W.; Erker, G. Reversible Metal-Free Carbon Dioxide Binding by Frustrated Lewis Pairs. *Angew. Chem., Int. Ed.* **2009**, *48*, 6643−6646.

(21) Stephan, D. W. Frustrated Lewis Pairs. *J. Am. Chem. Soc.* **2015**, *137*, 10018−10032.

(22) Dureen, M. A.; Stephan, D. W. Reactions of Boron Amidinates with CO_2 and CO and Other Small Molecules. *J. Am. Chem. Soc.* **2010**, *132*, 13559−13568.

(23) Theuergarten, E.; Schlüns, D.; Grunenberg, J.; Daniliuc, C. G.; Jones, P. G.; Tamm, M. Intramolecular heterolytic dihydrogen cleavage by a bifunctional frustrated pyrazolylborane Lewis pair. *Chem. Commun.* **2010**, *46*, 8561−8563.

(24) von Grotthuss, E.; Diefenbach, M.; Bolte, M.; Lerner, H.-W.; Holthausen, M. C.; Wagner, M. Reversible Dihydrogen Activation by Reduced Aryl Boranes as Main-Group Ambiphiles. *Angew. Chem., Int. Ed.* **2016**, *55*, 14067−14071.

(25) Lu, G.; Li, H.; Zhao, L.; Huang, F.; Schleyer, P. v. R.; Wang, Z.-X. Designing Metal-Free Catalysts by Mimicking Transition-Metal Pincer Templates. *Chem. − Eur. J.* **2011**, *17*, 2038−2043.

(26) Devillard, M.; Alvarez Lamsfus, C. A.; Vreeken, V.; Maron, L.; van der Vlugt, J. I. Versatile coordination of a reactive P,N-ligand toward boron, aluminum and gallium and interconversion reactivity. *Dalton Trans.* **2016**, *45*, 10989−10998.

(27) Gellrich, U.; Diskin-Posner, Y.; Shimon, L. J. W.; Milstein, D. Reversible Aromaticity Transfer in a Bora-Cycle: Boron−Ligand Cooperation. *J. Am. Chem. Soc.* **2016**, *138*, 13307−13313.

(28) Gellrich, U. Reversible Hydrogen Activation by a Pyridonate Borane Complex: Combining Frustrated Lewis Pair Reactivity with Boron-Ligand Cooperation. *Angew. Chem., Int. Ed.* **2018**, *57*, 4779−4782.

(29) Wech, F.; Gellrich, U. Hydrogenation of Olefins, Alkynes, Allenes, and Arenes by Borane-Based Frustrated Lewis Pairs. *Synthesis* **2022**, *54*, 3421−3431.
(30) Hasenbeck, M.; Müller, T.; Gellrich, U. Metal-free *gem* selective dimerization of terminal alkynes catalyzed by a pyridonate borane complex. *Catal. Sci. Technol.* **2019**, *9*, 2438−2444.
(31) Hasenbeck, M.; Ahles, S.; Averdunk, A.; Becker, J.; Gellrich, U. Formation of Nucleophilic Allylboranes from Molecular Hydrogen and Allenes Catalyzed by a Pyridonate Borane that Displays Frustrated Lewis Pair Reactivity. *Angew. Chem., Int. Ed.* **2020**, *59*, 23885−23891.
(32) Wech, F.; Hasenbeck, M.; Gellrich, U. Semihydrogenation of Alkynes Catalyzed by a Pyridone Borane Complex: Frustrated Lewis Pair Reactivity and Boron−Ligand Cooperation in Concert. *Chem. − Eur. J.* **2020**, *26*, 13445−13450.
(33) Wech, F.; Müller, T.; Becker, J.; Gellrich, U. Synthesis of 6-Adamantyl-2-pyridone and Reversible Hydrogen Activation by the Corresponding Bis(perfluorophenyl)Borane Complex. *Synthesis* **2021**, *53*, 666−672.
(34) Stephan, D. W.; Erker, G. Frustrated Lewis Pair Chemistry: Development and Perspectives. *Angew. Chem., Int. Ed.* **2015**, *54*, 6400−6441.
(35) Khan, M. N.; van Ingen, Y.; Boruah, T.; McLauchlan, A.; Wirth, T.; Melen, R. L. Advances in CO_2 activation by frustrated Lewis pairs: from stoichiometric to catalytic reactions. *Chem. Sci.* **2023**, *14*, 13661−13695.
(36) Waerder, B.; Pieper, M.; Körte, L. A.; Kinder, T. A.; Mix, A.; Neumann, B.; Stammler, H.-G.; Mitzel, N. W. A Neutral Silicon/Phosphorus Frustrated Lewis Pair. *Angew. Chem., Int. Ed.* **2015**, *54*, 13416−13419.
(37) Barnett, B. R.; Moore, C. E.; Rheingold, A. L.; Figueroa, J. S. Frustrated Lewis pair behavior of monomeric (boryl)iminomethanes accessed from isocyanide 1,1-hydroboration. *Chem. Commun.* **2015**, *51*, 541−544.
(38) Stoy, A.; Böhnke, J.; Jiménez-Halla, J. O. C.; Dewhurst, R. D.; Thiess, T.; Braunschweig, H. CO_2 Binding and Splitting by Boron−Boron Multiple Bonds. *Angew. Chem., Int. Ed.* **2018**, *57*, 5947−5951.
(39) Ishida, N.; Okumura, S.; Kawasaki, T.; Murakami, M. 2-Arylsilacyclobutane as a Latent Carbanion Reacting with CO_2. *Angew. Chem., Int. Ed.* **2018**, *57*, 11399−11403.
(40) Weetman, C.; Bag, P.; Szilvási, T.; Jandl, C.; Inoue, S. CO_2 Fixation and Catalytic Reduction by a Neutral Aluminum Double Bond. *Angew. Chem., Int. Ed.* **2019**, *58*, 10961−10965.
(41) Stoy, A.; Härterich, M.; Dewhurst, R. D.; Jiménez-Halla, J. O. C.; Endres, P.; Eyßelein, M.; Kupfer, T.; Deissenberger, A.; Thiess, T.; Braunschweig, H. Evidence for Borylene Carbonyl (LHB═C═O) and Base-Stabilized (LHB═O) and Base-Free Oxoborane (RB≡O) Intermediates in the Reactions of Diborenes with CO_2. *J. Am. Chem. Soc.* **2022**, *144*, 3376−3380.
(42) Wentz, K. E.; Molino, A.; Freeman, L. A.; Dickie, D. A.; Wilson, D. J. D.; Gilliard, R. J., Jr. Activation of Carbon Dioxide by 9-Carbene-9-borafluorene Monoanion: Carbon Monoxide Releasing Transformation of Trioxaborinanone to Luminescent Dioxaborinanone. *J. Am. Chem. Soc.* **2022**, *144*, 16276−16281.
(43) Wilm, L. F. B.; Das, M.; Janssen-Müller, D.; Mück-Lichtenfeld, C.; Glorius, F.; Dielmann, F. Photoswitchable Nitrogen Superbases: Using Light for Reversible Carbon Dioxide Capture. *Angew. Chem., Int. Ed.* **2022**, *61*, No. e202112344.
(44) Xu, H.; Kostenko, A.; Weetman, C.; Fujimori, S.; Inoue, S. An Aluminum Telluride with a Terminal Al═Te Bond and its Conversion to an Aluminum Tellurocarbonate by CO_2 Reduction. *Angew. Chem., Int. Ed.* **2023**, *62*, No. e202216021.
(45) Groll, L.; Kelly, J. A.; Inoue, S. Reactivity of NHI-Stabilized Heavier Tetrylenes towards CO_2 and N_2O. *Chem. Asian J.* **2024**, *19*, No. e202300941.
(46) Thömmes, A.-L.; Völker, R.; Morgenstern, B.; Zimmer, M.; Munz, D.; Kay, C. W. M.; Scheschkewitz, D. Silagermylenation of C═O bonds and radical fragmentation of CO2-expanded bis(germylene) by a cyclic (alkyl)(amino)carbene. *Inorg. Chem. Front.* **2025**, *12*, 4835−4843.
(47) Kiefer, F. J.; Kostenko, A.; Holzner, R.; Inoue, S. Reversible CO Insertion into the Si = Si Double Bond Enables a Disila-Bislactone Formation via Subsequent CO_2 Addition. *J. Am. Chem. Soc.* **2025**, *147*, 26663−26673.
(48) Theuergarten, E.; Schlösser, J.; Schlüns, D.; Freytag, M.; Daniliuc, C. G.; Jones, P. G.; Tamm, M. Fixation of carbon dioxide and related small molecules by a bifunctional frustrated pyrazolylborane Lewis pair. *Dalton Trans.* **2012**, *41*, 9101−9110.
(49) Wu, D.; Kong, L.; Li, Y.; Ganguly, R.; Kinjo, R. 1,3,2,5-Diazadiborinine featuring nucleophilic and electrophilic boron centres. *Nat. Commun.* **2015**, *6*, No. 7340.
(50) Sigmund, L. M.; Engels, E.; Richert, N.; Greb, L. Calix[4]-pyrrolato gallate: square planar-coordinated gallium(III) and its metal−ligand cooperative reactivity with CO_2 and alcohols. *Chem. Sci.* **2022**, *13*, 11215−11220.
(51) Barker, J. E.; Obi, A. D.; Dickie, D. A.; Gilliard, R. J., Jr. Boron-Doped Pentacenes: Isolation of Crystalline 5,12- and 5,7-Diboratapentacene Dianions. *J. Am. Chem. Soc.* **2023**, *145*, 2028−2034.
(52) Chen, X.; Yang, Y.; Wang, H.; Mo, Z. Cooperative Bond Activation and Catalytic CO_2 Functionalization with a Geometrically Constrained Bis(silylene)-Stabilized Borylene. *J. Am. Chem. Soc.* **2023**, *145*, 7011−7020.
(53) Huff, C. A.; Kampf, J. W.; Sanford, M. S. Role of a Noninnocent Pincer Ligand in the Activation of CO_2 at (PNN)Ru(H)(CO). *Organometallics* **2012**, *31*, 4643−4645.
(54) Vogt, M.; Gargir, M.; Iron, M. A.; Diskin-Posner, Y.; Ben-David, Y.; Milstein, D. A New Mode of Activation of CO_2 by Metal−Ligand Cooperation with Reversible C−C and M−O Bond Formation at Ambient Temperature. *Chem. − Eur. J.* **2012**, *18*, 9194−9197.
(55) Vogt, M.; Nerush, A.; Diskin-Posner, Y.; Ben-David, Y.; Milstein, D. Reversible CO_2 binding triggered by metal−ligand cooperation in a rhenium(I) PNP pincer-type complex and the reaction with dihydrogen. *Chem. Sci.* **2014**, *5*, 2043−2051.
(56) Feller, M.; Gellrich, U.; Anaby, A.; Diskin-Posner, Y.; Milstein, D. Reductive Cleavage of CO_2 by Metal−Ligand-Cooperation Mediated by an Iridium Pincer Complex. *J. Am. Chem. Soc.* **2016**, *138*, 6445−6454.
(57) Ferrer, M.; Alkorta, I.; Elguero, J.; Oliva-Enrich, J. M. (Pyridin-2-ylmethyl)triel Derivatives as Masked Frustrated Lewis Pairs. Interactions and CO_2-Sequestration. *ChemPhysChem* **2024**, *25*, No. e202300750.
(58) He, G.; Shynkaruk, O.; Lui, M. W.; Rivard, E. Small Inorganic Rings in the 21st Century: From Fleeting Intermediates to Novel Isolable Entities. *Chem. Rev.* **2014**, *114*, 7815−7880.
(59) Fontana, N.; Espinosa-Jalapa, N. A.; Seidl, M.; Bauer, J. O. Easy Access to Enantiomerically Pure Heterocyclic Silicon-Chiral Phosphonium Cations and the Matched/Mismatched Case of Dihydrogen Release. *Chem. − Eur. J.* **2021**, *27*, 2649−2653.
(60) Fontana, N.; Espinosa-Jalapa, N. A.; Seidl, M.; Bauer, J. O. Hidden silylium-type reactivity of a siloxane-based phosphonium−hydroborate ion pair. *Chem. Commun.* **2022**, *58*, 2144−2147.
(61) Falk, A.; Bauer, J. O. Structural and Electronic Effects on Phosphine Chalcogenide Stabilized Silicon Centers in Four-Membered Heterocyclic Cations. *Inorg. Chem.* **2022**, *61*, 15576−15588.
(62) Fontana, N.; Bauer, J. O. A Cyclic Phosphonium Ion with an Asymmetrically Substituted Selenide-Stabilized Silicon Center: Synthesis, Structure, and Substituent Effects. *ChemistrySelect* **2023**, *8*, No. e202301373.
(63) Ott, H.; Pieper, U.; Leusser, D.; Flierler, U.; Henn, J.; Stalke, D. Carbanion or Amide? First Charge Density Study of Parent 2-Picolyllithium. *Angew. Chem., Int. Ed.* **2009**, *48*, 2978−2982.
(64) Kennedy, A. R.; Mulvey, R. E.; Urquhart, R. I.; Robertson, S. D. Lithium, sodium and potassium picolyl complexes: syntheses, structures and bonding. *Dalton Trans.* **2014**, *43*, 14265−14274.

https://doi.org/10.1021/jacs.5c16770
J. Am. Chem. Soc. 2025, 147, 47573−47583

(65) Brouillet, E. V.; Kennedy, A. R.; Krämer, T.; Mulvey, R. E.; Robertson, S. D.; Stewart, A.; Towie, S. Synthesis, Structure, and DFT Analysis of the THF Solvate of 2-Picolyllithium: A 2-Picolyllithium Solvate with Significant Carbanionic Character. *Z. Anorg. Allg. Chem.* **2020**, *646*, 726−733.
(66) Colgan, D.; Papasergio, R. I.; Raston, C. L.; White, A. H. Lithium(η^3-aza-allyl) Type Complexes derived from the Metallation of 2-$(Me_3Si)_{3-n}$ $CH_nC_5H_4N$; Influence of Solvent and Degree of Substitution, n = 1 or 2, on the Nature of the Product. *J. Chem. Soc., Chem. Commun.* **1984**, 1708−1710.
(67) Papasergio, R. I.; Skelton, B. W.; Twiss, P.; White, A. H.; Raston, C. L. Lithiation of 2-$Me_3SiCHRC_5H_4N$(R = H or $SiMe_3$): influence of solvent on the nature of the product (from *X*-ray structure determinations) and asymmetric induction. A note on the lithiation of some analogous 3- and 4-methylpyridines. *J. Chem. Soc., Dalton Trans.* **1990**, 1161−1172.
(68) Jones, C.; Kennard, C. H. L.; Raston, C. L.; Smith, G. Negative hyperconjugation control of acidities in α-trimethylsilyl substituted α-picolines: isolation of $[Li\{NC_5H_4\text{-}2\text{-}C(H)(SiMe_3)_2\}\{NC_5H_4\text{-}2\text{-}C(H)(SiMe_3)\}]_2$. *J. Organomet. Chem.* **1990**, *396*, C39−C42.
(69) van den Ancker, T. R.; Raston, C. L. Main Group and Group 11, 12, 2-pyridyl-(trimethylsilyl)methyl and -bis(trimethylsilyl)-methyl chemistry. *J. Organomet. Chem.* **1995**, *500*, 289−297.
(70) Scherer, W.; Sirsch, P.; Grosche, M.; Spiegler, M.; Mason, S. A.; Gardiner, M. G. Agostic deformations based on electron delocalization in the alkyllithium-complex $[\{2\text{-}(Me_3Si)_2CLiC_5H_4N\}_2$. *Chem. Commun.* **2001**, 2072−2073.
(71) McLellan, R.; Kennedy, A. R.; Orr, S. A.; Robertson, S. D.; Mulvey, R. E. Lithium Dihydropyridine Dehydrogenation Catalysis: A Group 1 Approach to the Cyclization of Diamine Boranes. *Angew. Chem., Int. Ed.* **2017**, *56*, 1036−1041.
(72) McLellan, R.; Kennedy, A. R.; Mulvey, R. E.; Orr, S. A.; Robertson, S. D. 1-Alkali-metal-2-alkyl-1,2-dihydropyridines: Soluble Hydride Surrogates for Catalytic Dehydrogenative Coupling and Hydroboration Applications. *Chem. − Eur. J.* **2017**, *23*, 16853−16861.
(73) Macdonald, P. A.; Banerjee, S.; Kennedy, A. R.; Mulvey, R. E.; Robertson, S. D. Structural characterization of the 1-metallo-2-*t*-butyl-1,2-dihydropyridyl rubidium and caesium complexes. *Polyhedron* **2023**, *234*, No. 116302.
(74) Macdonald, P. A.; Banerjee, S.; Kennedy, A. R.; van Teijlingen, A.; Robertson, S. D.; Tuttle, T.; Mulvey, R. E. Alkali Metal Dihydropyridines in Transfer Hydrogenation Catalysis of Imines: Amide Basicity versus Hydride Surrogacy. *Angew. Chem., Int. Ed.* **2023**, *62*, No. e202304966.
(75) Macdonald, P. A.; Kennedy, A. R.; Weetman, C. E.; Robertson, S. D.; Mulvey, R. E. Synthesis, characterisation, and catalytic application of a soluble molecular carrier of sodium hydride activated by a substituted 4-(dimethylamino)pyridine. *Commun. Chem.* **2024**, *7*, No. 94.
(76) Vergnaud, J.; Ayed, T.; Hussein, K.; Vendier, L.; Grellier, M.; Bouhadir, G.; Barthelat, J.-C.; Sabo-Etienne, S.; Bourissou, D. Synthesis, structure and coordination of the ambiphilic ligand (2-picolyl)BCy_2. *Dalton Trans.* **2007**, 2370−2372.
(77) Son, J.-H.; Hoefelmeyer, J. D. 1,2-Nucleophilic addition of 2-(picolyl)organoboranes to nitrile, aldehyde, ketone, and amide. *Org. Biomol. Chem.* **2012**, *10*, 6656−6664.
(78) Körte, L. A.; Warner, R.; Vishnevskiy, Y. V.; Neumann, B.; Stammler, H.-G.; Mitzel, N. W. Intramolecular pyridine-based frustrated Lewis-pairs. *Dalton Trans.* **2015**, *44*, 9992−10002.
(79) Zheng, J.; Lin, Y.-J.; Wang, H. Synthesis of 2-(lutidinyl)-organoboranes and their reactivities against dihydrogen and pinacol borane. *Dalton Trans.* **2016**, *45*, 6088−6093.
(80) Allen, F. H.; Kennard, O.; Watson, D. G.; Brammer, L.; Orpen, A. G.; Taylor, R. Tables of Bond Lengths determined by *X*-Ray and Neutron Diffraction. Part 1. Bond Lengths in Organic Compounds. *J. Chem. Soc., Perkin Trans. 2* **1987**, *2*, S1−S19.
(81) Brook, A. G.; MacRae, D. M.; Limburg, W. W. Stereochemistry of the Formation and Thermal Rearrangement of β-Ketosilanes. *J. Am. Chem. Soc.* **1967**, *89*, 5493−5495.
(82) Brook, A. G. Some Molecular Rearrangements of Organosilicon Compounds. *Acc. Chem. Res.* **1974**, *7*, 77−84.
(83) All computed, geometry-optimized structures of the boryl silyl ketene acetals likewise display a pronounced shortening of the C−O bond within the C−O−B unit compared to the corresponding bond in the C−O−Si unit (for details, see Section S5 in the SI.
(84) Weinhold, F.; West, R. The Nature of the Silicon-Oxygen Bond. *Organometallics* **2011**, *30*, 5815−5824.
(85) Weinhold, F.; West, R. Hyperconjugative Interactions in Permethylated Siloxanes and Ethers: The Nature of the SiO Bond. *J. Am. Chem. Soc.* **2013**, *135*, 5762−5767.
(86) Bauer, J. O. Influence of Amino Functions on the Coordination Ability of Silyl Ethers and Disiloxanes. *Organometallics* **2022**, *41*, 321−327.
(87) Zhao, Y.; Truhlar, D. G. The M06 suite of density functionals for main group thermochemistry, thermochemical kinetics, noncovalent interactions, excited states, and transition elements: two new functionals and systematic testing of four M06-class functionals and 12 other functionals. *Theor. Chem. Acc.* **2008**, *120*, 215−241.
(88) Krishnan, R.; Binkley, J. S.; Seeger, R.; Pople, J. A. Self-consistent molecular orbital methods. XX. A basis set for correlated wave functions. *J. Chem. Phys.* **1980**, *72*, 650−654.
(89) McLean, A. D.; Chandler, G. S. Contracted Gaussian basis sets for molecular calculations. I. Second row atoms, Z = 11−18. *J. Chem. Phys.* **1980**, *72*, 5639−5648.
(90) Clark, T.; Chandrasekhar, J.; Spitznagel, G. W.; Schleyer, P. v. R. Efficient Diffuse Function-Augmented Basis Sets for Anion Calculations. III. The 3−21+G Basis Set for First-Row Elements, Li−F. *J. Comput. Chem.* **1983**, *4*, 294−301.
(91) Frisch, M. J.; Trucks, G. W.; Schlegel, H. B.; Scuseria, G. E.; Robb, M. A.; Cheeseman, J. R.; Scalmani, G.; Barone, V.; Mennucci, B.; Petersson, G. A.; Nakatsuji, H.; Caricato, M.; Li, X.; Hratchian, H. P.; Izmaylov, A. F.; Bloino, J.; Zheng, G.; Sonnenberg, J. L.; Hada, M.; Ehara, M.; Toyota, K.; Fukuda, R.; Hasegawa, J.; Ishida, M.; Nakajima, T.; Honda, Y.; Kitao, O.; Nakai, H.; Vreven, T.; Montgomery, J. A., Jr.; Peralta, J. E.; Ogliaro, F.; Bearpark, M.; Heyd, J. J.; Brothers, E.; Kudin, K. N.; Staroverov, V. N.; Keith, T.; Kobayashi, R.; Normand, J.; Raghavachari, K.; Rendell, A.; Burant, J. C.; Iyengar, S. S.; Tomasi, J.; Cossi, M.; Rega, N.; Millam, J. M.; Klene, M.; Knox, J. E.; Cross, J. B.; Bakken, V.; Adamo, C.; Jaramillo, J.; Gomperts, R.; Stratmann, R. E.; Yazyev, O.; Austin, A. J.; Cammi, R.; Pomelli, C.; Ochterski, J. W.; Martin, R. L.; Morokuma, K.; Zakrzewski, V. G.; Voth, G. A.; Salvador, P.; Dannenberg, J. J.; Dapprich, S.; Daniels, A. D.; Farkas, O.; Foresman, J. B.; Ortiz, J. V.; Cioslowski, J.; Fox, D. J. *Gaussian 09. Revision E.01*; Gaussian, Inc.: Wallingford, CT, USA, 2013.
(92) Tomasi, J.; Mennucci, B.; Cammi, R. Quantum Mechanical Continuum Solvation Models. *Chem. Rev.* **2005**, *105*, 2999−3093.
(93) Takahashi, M.; Kira, M. A Theoretical Study of Mechanisms of 1,3-Silyl Migration in Formylmethylsilane and Related Migrations. Comparison with Allylsilane. *J. Am. Chem. Soc.* **1999**, *121*, 8597−8603.
(94) Jiang, X.; Wang, R. Recent Developments in Catalytic Asymmetric Inverse-Electron-Demand Diels−Alder Reaction. *Chem. Rev.* **2013**, *113*, 5515−5546.
(95) Foster, R. A. A.; Willis, M. C. Tandem *inverse*-electron-demand *hetero-/retro*-Diels−Alder reactions for aromatic nitrogen heterocycle synthesis. *Chem. Soc. Rev.* **2013**, *42*, 63−76.
(96) Knall, A.-C.; Slugovc, C. Inverse electron demand Diels−Alder (iEDDA)-initiated conjugation: a (high) potential click chemistry scheme. *Chem. Soc. Rev.* **2013**, *42*, 5131−5142.
(97) Oliveira, B. L.; Guo, Z.; Bernardes, G. J. L. Inverse electron demand Diels−Alder reactions in chemical biology. *Chem. Soc. Rev.* **2017**, *46*, 4895−4950.
(98) Png, Z. M.; Zeng, H.; Ye, Q.; Xu, J. Inverse-Electron-Demand Diels−Alder Reactions: Principles and Applications. *Chem. − Asian J.* **2017**, *12*, 2142−2159.
(99) Zhang, J.; Shukla, V.; Boger, D. L. Inverse Electron Demand Diels−Alder Reactions of Heterocyclic Azadienes, 1-Aza-1,3-Buta-

dienes, Cyclopropenone Ketals, and Related Systems. A Retrospective. *J. Org. Chem.* **2019**, *84*, 9397−9445.
(100) Narasaka, K.; Soai, K.; Mukaiyama, T. The new Michael reaction. *Chem. Lett.* **1974**, *3*, 1223−1224.
(101) Mukaiyama, T. Titanium Tetrachloride in Organic Synthesis. *Angew. Chem., Int. Ed.* **1977**, *16*, 817−826.
(102) Borths, C. J.; Carrera, D. E.; MacMillan, D. W. C. Development of a general, enantioselective organocatalytic Mukaiyama−Michael reaction with α,β-unsaturated aldehydes. *Tetrahedron* **2009**, *65*, 6746−6753.
(103) Gatzenmeier, T.; Kaib, P. S. J.; Lingnau, J. B.; Goddard, R.; List, B. The Catalytic Asymmetric Mukaiyama−Michael Reaction of Silyl Ketene Acetals with α,β-Unsaturated Methyl Esters. *Angew. Chem., Int. Ed.* **2018**, *57*, 2464−2468.
(104) Palomo, C.; Oiarbide, M.; García, J. M. The Aldol Addition Reaction: An Old Transformation at Constant Rebirth. *Chem.−Eur. J.* **2002**, *8*, 36−44.
(105) Kan, S. B. J.; Ng, K. K.-H.; Paterson, I. The Impact of the Mukaiyama Aldol Reaction in Total Synthesis. *Angew. Chem., Int. Ed.* **2013**, *52*, 9097−9108.
(106) Matsuo, J.-i.; Murakami, M. The Mukaiyama Aldol Reaction: 40 Years of Continuous Development. *Angew. Chem., Int. Ed.* **2013**, *52*, 9109−9118.
(107) Mukaiyama, T.; Inomata, K.; Muraki, M. Vinyloxyboranes as Synthetic Intermediates. *J. Am. Chem. Soc.* **1973**, *95*, 967−968.
(108) Mukaiyama, T.; Banno, K.; Narasaka, K. New Cross-Aldol Reactions. Reactions of Silyl Enol Ethers with Carbonyl Compounds Activated by Titanium Tetrachloride. *J. Am. Chem. Soc.* **1974**, *96*, 7503−7509.
(109) Mukaiyama, T. Explorations into New Reaction Chemistry. *Angew. Chem., Int. Ed.* **2004**, *43*, 5590−5614.
(110) Heathcock, C. H.; Davidsen, S. K.; Hug, K. T.; Flippin, L. A. Acyclic Stereoselection. 36. Simple Diastereoselection in the Lewis Acid Mediated Reactions of Enol Silanes with Aldehydes. *J. Org. Chem.* **1986**, *51*, 3027−3037.
(111) Denmark, S. E.; Lee, W. Investigations on Transition-State Geometry in the Lewis Acid- (Mukaiyama) and Fluoride-Promoted Aldol Reactions. *J. Org. Chem.* **1994**, *59*, 707−709.
(112) Lee, J. M.; Helquist, P.; Wiest, O. Diastereoselectivity in Lewis-Acid-Catalyzed Mukaiyama Aldol Reactions: A DFT Study. *J. Am. Chem. Soc.* **2012**, *134*, 14973−14981.
(113) Zimmerman, H. E.; Traxler, M. D. The Stereochemistry of the Ivanov and Reformatsky Reactions. I. *J. Am. Chem. Soc.* **1957**, *79*, 1920−1923.
(114) Chan, A. P. Y.; Sergeev, A. G. Metal-mediated cleavage of unsaturated C-C bonds. *Coord. Chem. Rev.* **2020**, *413*, No. 213213.
(115) Liang, Y.-F.; Bilal, M.; Tang, L.-Y.; Wang, T.-Z.; Guan, Y.-Q.; Cheng, Z.; Zhu, M.; Wei, J.; Jiao, N. Carbon−Carbon Bond Cleavage for Late-Stage Functionalization. *Chem. Rev.* **2023**, *123*, 12313−12370.
(116) Grubbs, R. H. Olefin metathesis. *Tetrahedron* **2004**, *60*, 7117−7140.
(117) *Handbook of Metathesis*; Grubbs, R. H.; Khosravi, E., Eds.; Wiley-VCH: Weinheim, Germany, 2015; Vol. *3*.
(118) Wang, T.; Jiao, N. TEMPO-catalyzed Aerobic Oxygenation and Nitrogenation of Olefins via C═C Double-Bond Cleavage. *J. Am. Chem. Soc.* **2013**, *135*, 11692−11695.
(119) Imada, Y.; Okada, Y.; Noguchi, K.; Chiba, K. Selective Functionalization of Styrenes with Oxygen Using Different Electrode Materials: Olefin Cleavage and Synthesis of Tetrahydrofuran Derivatives. *Angew. Chem., Int. Ed.* **2019**, *58*, 125−129.
(120) Salzmann, K.; Segarra, C.; Albrecht, M. Donor-Flexible Bis(pyridylidene amide) Ligands for Highly Efficient Ruthenium-Catalyzed Olefin Oxidation. *Angew. Chem., Int. Ed.* **2020**, *59*, 8932−8936.
(121) Huang, Z.; Guan, R.; Shanmugam, M.; Bennett, E. L.; Robertson, C. M.; Brookfield, A.; McInnes, E. J. L.; Xiao, J. Oxidative Cleavage of Alkenes by O_2 with a Non-Heme Manganese Catalyst. *J. Am. Chem. Soc.* **2021**, *143*, 10005−10013.
(122) Ruffoni, A.; Hampton, C.; Simonetti, M.; Leonori, D. Photoexcited nitroarenes for the oxidative cleavage of alkenes. *Nature* **2022**, *610*, 81−86.
(123) Wise, D. E.; Gogarnoiu, E. S.; Duke, A. D.; Paolillo, J. M.; Vacala, T. L.; Hussain, W. A.; Parasram, M. Photoinduced Oxygen Transfer Using Nitroarenes for the Anaerobic Cleavage of Alkenes. *J. Am. Chem. Soc.* **2022**, *144*, 15437−15442.
(124) Xue, W.; Jiang, Y.; Lu, H.; You, B.; Wang, X.; Tang, C. Direct C−C Double Bond Cleavage of Alkenes Enabled by Highly Dispersed Cobalt Catalyst and Hydroxylamine. *Angew. Chem., Int. Ed.* **2023**, *62*, No. e202314364.
(125) Schmidt-Räntsch, T.; Verplancke, H.; Kehl, A.; Sun, J.; Bennati, M.; Holthausen, M. C.; Schneider, S. C═C Dissociative Imination of Styrenes by a Photogenerated Metallonitrene. *JACS Au* **2024**, *4*, 3421−3426.
(126) Hafner, K.; Häfner, K. H.; König, C.; Kreuder, M.; Ploss, G.; Schulz, G.; Sturm, E.; Vöpel, K. H. Fulvenes as Isomers of Benzenoid Compounds. *Angew. Chem., Int. Ed.* **1963**, *2*, 123−134.
(127) Bergmann, E. D. Fulvenes and Substituted Fulvenes. *Chem. Rev.* **1968**, *68*, 41−84.
(128) Joseph, J.; Preethalayam, P.; Radhakrishnan, K. V.; Jaroschik, F.; Vasse, J.-L. Titanium and Zirconium Hydride-Catalyzed Regioselective Isomerization of 1,4-Dihydrofulvenes: Access to 1-Substituted 1,2-Dihydrofulvenes. *Org. Lett.* **2015**, *17*, 6202−6205.
(129) Aguilar, E.; Sanz, R.; Fernández-Rodríguez, M. A.; García-García, P. 1,3-Dien-5-ynes: Versatile Building Blocks for the Synthesis of Carbo- and Heterocycles. *Chem. Rev.* **2016**, *116*, 8256−8311.
(130) Preethalayam, P.; Krishnan, K. S.; Thulasi, S.; Chand, S. S.; Joseph, J.; Nair, V.; Jaroschik, F.; Radhakrishnan, K. V. Recent Advances in the Chemistry of Pentafulvenes. *Chem. Rev.* **2017**, *117*, 3930−3989.

https://doi.org/10.1021/jacs.5c16770
J. Am. Chem. Soc. 2025, 147, 47573−47583